Published in Journal of Non-Crystalline Solids 266-269, 1114-1118, 2000
which should be used for any reference to this work


# Electronic transport in hydrogenated microcrystalline silicon: similarities with amorphous silicon

C. Droz *, M. Goerlitzer, N. Wyrsch, A. Shah

*Institute of Microtechnology, University of Neuchâtel, Breguet 2, CH-2000 Neuchâtel, Switzerland*

**Abstract**

Undoped hydrogenated microcrystalline silicon (μc-Si:H) layers were grown by the very high frequency glow discharge (VHF-GD) technique under various deposition conditions. The electronic transport properties under illumination were investigated by means of steady-state photoconductivity and steady-state photocarrier grating methods. Similarly to hydrogenated amorphous silicon (a-Si:H), power law dependencies as a function of the generation rate are observed for the photoconductivity, for the ambipolar diffusion length, and for the parameter $b$ (indicating the Fermi level). For μc-Si:H, as for a-Si:H, nearly constant product of (mobility×recombination time) of majority and minority carriers is observed as a function of the parameter $b$. Based on these similarities, we assume that the electronic transport model developed for a-Si:H remains valid for μc-Si:H.

## 1. Introduction

Hydrogenated microcrystalline silicon (μc-Si:H) has been successfully incorporated as intrinsic layer in p–i–n ($\eta = 8.5\%$, [1]) or n–i–p ($\eta = 7.8\%$, [2]) solar cells. To achieve such a good collection in the cell, high mobility and recombination time (i.e. $\mu^0\tau^R$ products) are required. We are therefore interested in studying the electronic transport properties of intrinsic μc-Si:H layers, in view of their incorporation into solar cells.

Unlike a-Si:H, where transport models have been successfully developed (e.g. [3]), no transport model is so far available for μc-Si:H to our knowledge. The goal of this paper is to compare the electronic transport properties of intrinsic μc-Si:H layers with those of intrinsic a-Si:H layers. In this approach, coplanar electronic transport under illumination will be analysed in μc-Si:H layers with the same tools as those used for a-Si:H: steady-state photoconductivity (SSPC) and steady-state photocarrier grating (SSPG) techniques. From the photoconductivity, $\sigma_{\text{photo}}$, as measured by SSPC, the $\mu^0\tau^R$ product of the majority carriers ($\mu^0\tau^R_{\text{Maj}}$) is deduced (Eq. (1)), whereas from the ambipolar diffusion length, $L_{\text{amb}}$, as measured by SSPG, the $\mu^0\tau^R$ product of the minority carriers ($\mu^0\tau^R_{\text{min}}$) is deduced from Eq. (2)

$$\sigma_{\text{photo}} = qG\left(\mu_n^0\tau_n^R + \mu_p^0\tau_p^R\right), \tag{1}$$

$$L_{\text{amb}}^2 = \frac{kT}{q}\,\frac{\mu_n^0\tau_n^R \times \mu_p^0\tau_p^R}{\mu_n^0\tau_n^R + \mu_p^0\tau_p^R}\,C, \tag{2}$$

* Corresponding author. Tel.: +41-32 718 3312; fax: +41-32 718 3201.
*E-mail address:* corinne.droz@imt.unine.ch (C. Droz).

where $q$ is the elementary charge, $G$ the generation rate, $kT$ the thermal energy, $C$ a correction factor [4], $\tau_n^R = n_f/G$, $\tau_p^R = p_f/G$ are the recombination times (i.e. the mean time to recombination), and $\mu_{n,p}^0$ are the band mobilities. Here, we do not purposely specify any recombination model. Thus, we can use these quantities to describe layer transport properties as well for μc-Si:H as for a-Si:H.

Whereas the application of the SSPC method to μc-Si:H layers does not cause any specific problem, the validity of the SSPG method is more critical. In the SSPG technique [5], the ratio ($\beta$) of two currents is determined: the first current is measured in the presence of optical interference with a grating period, $\Lambda$, and the second current is measured without interference. The so-called 'Balberg plot' ($1/\Lambda^2$ as a function of $\sqrt{2/(1-\beta)}$) obtained thereby must be a linear function to evaluate $L_{amb}$ from the intersection of this line with the $y$-axis. However, the Balberg plot of μc-Si:H samples is usually not linear, but curved. We conjecture that this non-linearity is due to the fact that in μc-Si:H the ambipolar condition is not assured for all considered grating periods. However, we can demonstrate [6] that $L_{amb}$ can still be correctly determined from region of the data which can be fit with a linear function (see Fig. 1).

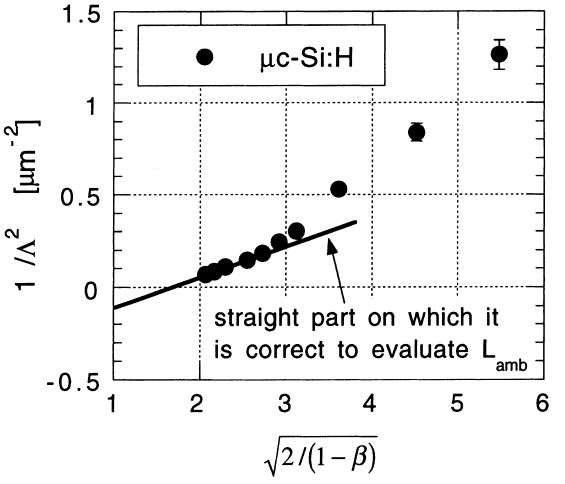


Fig. 1. Typical 'Balberg plot' obtained when measuring μc-Si:H samples by the SSPG method, with a generation rate $G \approx 4 \times 10^{20}$ cm$^{-3}$ s$^{-1}$. Note the deviation from a linear function. The ambipolar diffusion length $L_{amb}$ can nevertheless be evaluated on the linear part.

Because of the strong unintentional incorporation of oxygen in μc-Si:H layers (both during and after deposition (postoxidation)), which depends on deposition conditions, the Fermi level is consequently changed and the interpretation of the transport properties can be a problem [7]. To overcome this problem, we introduced the parameter $b$, which was defined as for a-Si:H as $b = \mu_n^0 n_f/\mu_p^0 p_f$ [4,8], where $n_f$ and $p_f$ are the free carriers densities. It is experimentally deduced from $\sigma_{photo}$ and $L_{amb}$ by setting

$$\frac{b}{(b+1)^2} = \frac{L_{amb}^2 q^2 G}{kT\sigma_{photo} C}. \tag{3}$$

Even if it is determined under non-equilibrium conditions, $b$ reflects the position of the Fermi level, $E_f$ ($b \approx 1$: $E_f$ midgap) [8], because the n- or p-type of the material is not changed by illumination. It is then possible to compare electronic transport in a-Si:H and in μc-Si:H, at a chosen value of $b$ (i.e. the same $n_f/p_f$ ratio, assuming the same band mobility ratio for both materials), and to compare μc-Si:H layers betweem them, since $b$ takes into account the shift in $E_f$ due to the postoxidation.

## 2. Experimental

All the samples in the present paper were produced by the VHF-GD technique [9] at frequencies between 70 and 130 MHz and effective deposition temperature of 220°C. To obtain nearly intrinsic μc-Si:H layers, a gas purifier was used [10]. Various concentrations of silane in hydrogen as well as various VHF-power were used. The films were deposited on glass (AF45 Schott) with a typical thickness of $2 \pm 0.5$ μm. While as-grown undoped μc-Si:H is a slightly n-type material, some samples were deposited with about 10 ppm of diborane to obtain slightly p-type μc-Si:H layers. Aluminium coplanar contacts were evaporated on the layers that were subsequently annealed at 180°C during 90 min. Both $\sigma_{photo}$ and $L_{amb}$ were simultaneously measured on each layer at room temperature and

with the same variable bias light intensity. A krypton laser ($\lambda = 647$ nm) was used as illumination source.

## 3. Results

The first similarity in transport between μc-Si:H and a-Si:H is in the power law dependencies of $L^2_{amb}$, $\sigma_{photo}$, and $b$ as a function of the generation rate, $G$. These power laws are shown in Fig. 2 for as-grown slightly n-type μc-Si:H as well as for slightly p-type doped μc-Si:H, for $G$ between $10^{19}$ and $10^{22}$ cm$^{-3}$ s$^{-1}$. The power law exponents $\gamma$ and $\lambda$ measured on μc-Si:H layers are in the same range as those measured on a-Si:H [6]. On the other hand, the exponent of $b$ ($\theta$) is usually negative for μc-Si:H, whereas it is in most cases positive for a-Si:H. Another representation of these power law dependencies on $G$ is given in Fig. 3, where $\mu^0\tau^R_{Maj}$ and $\mu^0\tau^R_{min}$, deduced from the $\sigma_{photo}$ and $L_{amb}$ of Fig. 2, are plotted as a function of $b$. Here, the change in $b$ is due to a change in $G$. Fig. 3, based on the same data of Fig. 2, reveals the strong dependency of $\sigma_{photo}$ on $G$, and the typical weak dependency of $L^2_{amb}$ with $G$. Fig. 3 also demonstrate the symmetry of the power law dependencies for the majority and minority free carriers in slightly p- and n-type μc-Si:H samples. Such a symmetry is not revealed in Fig. 2.

It has been observed [4,11] that, in the case of a series of slightly doped a-Si:H layers, the $\mu^0\tau^R$ products of the majority and minority carriers, when plotted as a function of $b$, display an anti-correlated behaviour (i.e. for a variation of the Fermi level (monitored by the parameter $b$) $\mu^0\tau^R_{Maj} \times \mu^0\tau^R_{min}$ is almost constant) for both slightly n-type ($b > 1$) and slightly p-type ($b < 1$) a-Si:H

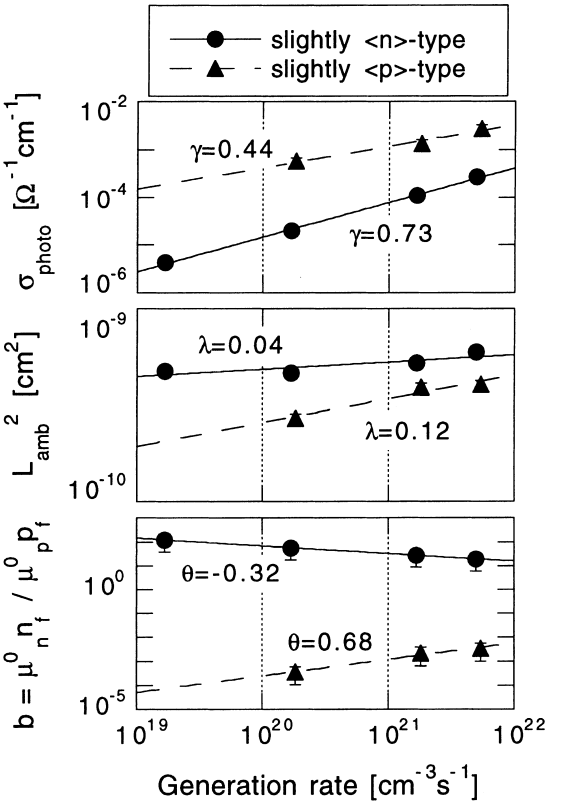


Fig. 2. Power law dependencies, and their fits, with the generation rate $G$ of the photoconductivity ($\sigma_{photo} \propto G^{\gamma}$), the ambipolar diffusion length ($L^2_{amb} \propto G^{\lambda}$), and the parameter $b$ ($b \propto G^{\theta}$), for a typical as-grown slightly n-type μc-Si:H layer and a typical slightly p-type μc-Si:H layer. Both layers were deposited with a silane concentration in hydrogen of 6%, the p-type layer was obtained by adding 10 ppm of diborane.

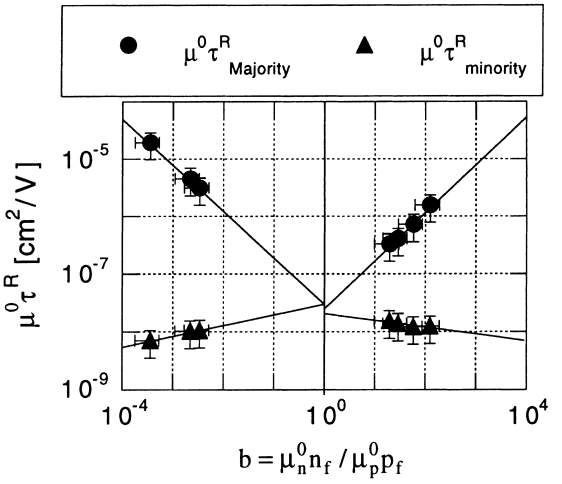


Fig. 3. $\mu^0\tau^R$ products of the majority carriers (as deduced from $\sigma_{photo}$) and of the minority carriers (as deduced from $L_{amb}$) as a function of the parameter $b$, representing the Fermi level position; data points (obtained by changing the generation rate) were taken from Fig. 2. This representation is symmetric for slightly n-type ($b > 1$) and p-type ($b < 1$) μc-Si:H layers. The lines are power law fits.

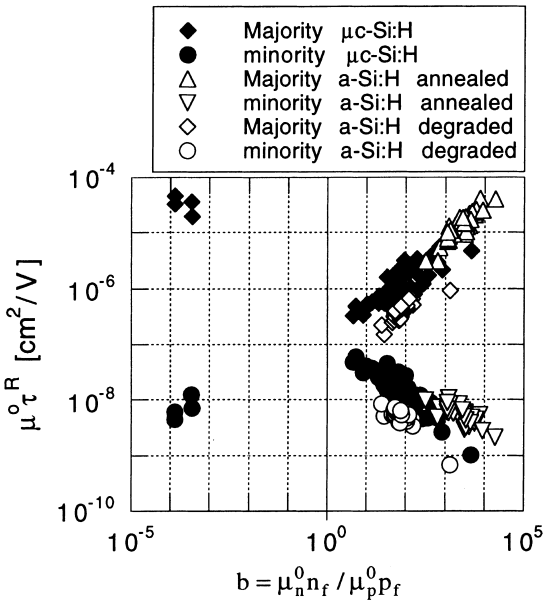


Fig. 4. Majority and minority $\mu^0\tau^R$ products measured on various μc-Si:H layers with a constant generation rate ($G \approx 2 \times 10^{20}$ cm$^{-3}$ s$^{-1}$), as a function of the parameter $b$. To quantitatively compare electronic transport in μc-Si:H and in a-Si:H, majority and minority $\mu^0\tau^R$ products measured on annealed ($G \approx 3 \times 10^{19}$ cm$^{-3}$s$^{-1}$) and degraded ($G \approx 2\times 10^{20}$ cm$^{-3}$s$^{-1}$) a-Si:H samples [14] are also represented.

materials. To compare μc-Si:H with a-Si:H, we have represented in Fig. 4 the $\mu^0\tau^R_{\mathrm{Maj}}$ and $\mu^0\tau^R_{\mathrm{min}}$ products, as a function of $b$, for μc-Si:H samples measured with a constant $G$. In other words, Fig. 4 is the plot of $\mu^0_n n_{\mathrm{f}}$ and $\mu^0_p p_{\mathrm{f}}$ vs $b$. The change in $b$ is here mainly due to unintentional incorporation of oxygen (during deposition or by postoxidation), which acts as a n-type dopant in μc-Si:H. Note that Fig. 4 only shows data for μc-Si:H samples for which the variation in the defect densities is less than a factor 10 (as deduced from the constant photocurrent method). In the case of μc-Si:H, as shown in Fig. 4, the behaviour of majority and minority carriers $\mu^0\tau^R$ products is surprisingly, as in a-Si:H, anticorrelated (i.e. $\mu^0_n n_{\mathrm{f}} \times \mu^0_p p_{\mathrm{f}} \approx$ constant). In Fig. 4 are also represented $\mu^0\tau^R_{\mathrm{Maj}}$ and $\mu^0\tau^R_{\mathrm{min}}$ products measured on various a-Si:H layers [12] in the annealed and degraded states. We remark that the $\mu^0\tau^R$ products of μc-Si:H samples are slightly larger than those of degraded a-Si:H samples, and are approximately equal to those of annealed a-Si:H layers.

## 4. Discussion

As shown in Fig. 4, the $\mu^0\tau^R$ products of the majority and minority carriers vary substantially with the Fermi level, represented here through the parameter $b$. When comparing electronic transport of various samples (μc-Si:H between them or μc-Si:H with a-Si:H), it is then crucial to know the position of the Fermi level. In this context, the use of the parameter $b$ is therefore essential for a correct interpretation of transport measurements.

The $\mu^0\tau^R$ products of majority and minority carriers measured on μc-Si:H samples show the same behaviours – power laws (Figs. 2 and 3) and correlations (Fig. 4) – as those observed on a-Si:H samples, and their values are within the same order of magnitude. We can thus postulate that the coplanar electronic transport under illumination in μc-Si:H material is similar to that in a-Si:H material. These similarities suggest that the electronic transport in μc-Si:H layers is governed by the amorphous phase present at the grain boundaries of μc-Si:H. Furthermore, this hypothesis sustains the idea of applying the transport model developed for a-Si:H [3] to μc-Si:H. In this model, the dangling bonds with their amphoteric character (i.e. three charge states) act as recombination centers, whereas the band tails act as traps. The recombination traffics of electrons and holes are related via their common recombination centers (i.e. the dangling bonds). As a consequence, the free carrier densities cannot vary independently. Indeed, conservation laws (generation equals recombination rate, charge neutrality) imply a relationship between the free carriers densities. Experimentally, this relationship translates into the anticorrelation of $\mu^0\tau^R$ products of the majority and minority carriers ($\mu^0_n n_{\mathrm{f}} \times \mu^0_p p_{\mathrm{f}} \approx$ constant), exactly as observed here for μc-Si:H layers (see Fig. 4).

Assuming that the recombination mechanism is similar in μc-Si:H and in a-Si:H, we can go one step further and apply to μc-Si:H the quality parameter $\mu^0\tau^0$ [13], introduced from the recombination model of a-Si:H, and used there to link the

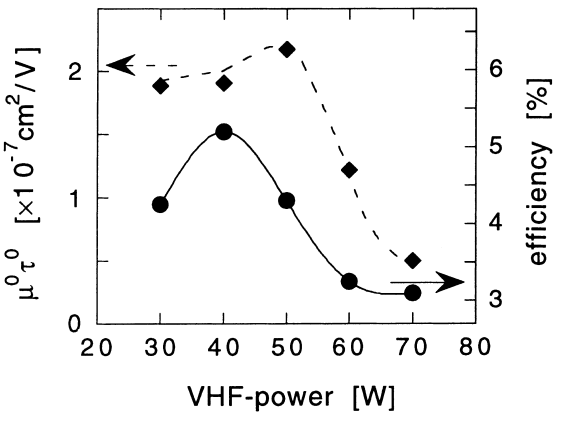


Fig. 5. Quality parameter $\mu^0\tau^0$ measured on a power series of μc-Si:H layers compared to the efficiencies of solar cells incorporating such layers as intrinsic layers (thickness = 3.5± 0.4 μm). The lines are only to guide the eye.

material quality with solar cell performance (as far as the latter is limited by the intrinsic layer). The quality parameter, $\mu^0\tau^0$, which is experimentally deduced from both $\mu^0\tau^R_{\mathrm{Maj}}$ and $\mu^0\tau^R_{\mathrm{min}}$ products, corresponds to the value which the measured $\mu^0\tau^R$ product would take if all dangling bonds in the material were neutral; $\mu^0\tau^0$ is independent of the Fermi level of the considered sample. Fig. 5 shows the $\mu^0\tau^0$ products for a series of μc-Si:H layers, obtained by changing the VHF-power, and compares them to the efficiencies of solar cells incorporating such layers as the intrinsic layer. This first successful attempt to correlate the quality of μc-Si:H layers with solar cell efficiencies strengthens the legitimacy to apply the transport model developed for a-Si:H to μc-Si:H.

Despite the remarkable similarities in the transport properties between μc-Si:H and a-Si:H, some significant differences still remain between these two materials. μc-Si:H is stable against light-soaking, whereas the properties of a-Si:H change with light. In p–i–n solar cells, the collection is exclusively controlled by drift in the case of a-Si:H cells, whereas a collection by drift and diffusion is observed in μc-Si:H cells [14]. A possible anisotropy of the transport properties in μc-Si:H could also mask a relation between the transport properties (based on coplanar measurements) and solar cell performance. However, a rough estimation for the latter from layer quality remains possible [15] as long as we mainly want to distinguish good material from bad material.

## 5. Conclusion

Electronic transport in coplanar configuration was evaluated on μc-Si:H layers from SSPC and SSPG techniques. From these measurements we evaluated the variations of the mobility and recombination time ($\mu^0\tau^R$) products of the majority and minority carriers as a function of $b$ (representing the Fermi level) for different generation rates and doping levels. The behaviours of the $\mu^0\tau^R$ products are similar in μc-Si:H as in a-Si:H. Therefore, we suggest to extend the electronic transport model developed for a-Si:H to μc-Si:H. The quality parameter $\mu^0\tau^0$ (based on the recombination model for a-Si:H), seems to match, even in μc-Si:H, with the solar cell performances. The use of the parameter $b$ allows us to directly compare transport properties in μc-Si:H and in a-Si:H. In this way, we conclude that electronic transport in μc-Si:H is slightly better than in a-Si:H.

## Acknowledgements

This work was supported by the Swiss National Science Foundation under grant FN-52337.

## References

[1] J. Meier, H. Keppner, S. Dubail, Y. Ziegler, L. Feitknecht, P. Torres, C. Hof, U. Kroll, D. Fischer, J. Cuperus, J.A. Anna Selvan, A. Shah, in: Proceedings of the Second WCPEC, Vienna, 1998, p. 375.
[2] L. Feitknecht, O. Kluth, Y. Ziegler, X. Niquille, P. Torres, J. Meier, N. Wyrsch, A. Shah, in: Proceedings of the 11th International PVSEC, 1999, to be published.
[3] J. Hubin, A. Shah, E. Sauvain, P. Pipoz, J. Appl. Phys. 78 (1995) 6050.
[4] E. Sauvain, PhD thesis, University of Neuchâtel, 1992.
[5] I. Balberg, Mater. Res. Soc. Symp. Proc. 258 (1992) 693.
[6] M. Goerlitzer, N. Beck, P. Torres, J. Meier, N. Wyrsch, A. Shah, J. Appl. Phys. 80 (1996) 5111.
[7] M. Goerlitzer, P. Torres, N. Beck, N. Wyrsch, H. Keppner, J. Pohl, A. Shah, J. Non-Cryst. Solids 227–230 (1998) 996.

[8] A. Shah, E. Sauvain, J. Hubin, P. Pipoz, C. Hof, Philos. Mag. B 75 (1997) 925.
[9] H. Curtins, N. Wyrsch, M. Favre, A. Shah, Plasma Chem. Plasma Proc. 7 (1987) 267.
[10] P. Torres, J. Meier, R. Flückiger, U. Kroll, J.A. Anna Selvan, H. Keppner, A. Shah, S.D. Littelwood, I.E. Kelly, P. Giannoulès, Appl. Phys. Lett. 69 (1996) 1373.
[11] N. Beck, A. Shah, N. Wyrsch, in: Proceedings of the First WCPEC, Hawaii, 1994, p. 476.
[12] Y. Ziegler, V. Daudrix, C. Droz, A. Shah, in: Proceedings of the 11th International PVSEC, 1999, to be published.
[13] N. Beck, N. Wyrsch, C. Hof, A. Shah, J. Appl. Phys. 79 (1996) 9361.
[14] N. Wyrsch, P. Torres, J. Meier, A. Shah, J. Non-Cryst. Solids 227–230 (1998) 1272.
[15] N. Wyrsch, L. Feitknecht, C. Droz, P. Torres, A. Shah, A. Poruba, M. Vanecek, these Proceedings, p. 1099.